



HAL
open science

Evaluating smartphone performance for cellular power measurement

Yanis Boussad, Leonardo Lizzi, Fabien Ferrero, Arnaud Legout

► **To cite this version:**

Yanis Boussad, Leonardo Lizzi, Fabien Ferrero, Arnaud Legout. Evaluating smartphone performance for cellular power measurement. [Research Report] UCA, Inria; UCA, LEAT. 2019. hal-02320342v1

HAL Id: hal-02320342

<https://inria.hal.science/hal-02320342v1>

Submitted on 21 Oct 2019 (v1), last revised 14 Apr 2020 (v3)

HAL is a multi-disciplinary open access archive for the deposit and dissemination of scientific research documents, whether they are published or not. The documents may come from teaching and research institutions in France or abroad, or from public or private research centers.

L'archive ouverte pluridisciplinaire **HAL**, est destinée au dépôt et à la diffusion de documents scientifiques de niveau recherche, publiés ou non, émanant des établissements d'enseignement et de recherche français ou étrangers, des laboratoires publics ou privés.

Evaluating smartphone performance for cellular power measurement

Yanis BOUSSAD

yanis.boussad@inria.fr
Université Côte d’Azur, Inria
Valbonne, France

Fabien Ferrero

fabien.ferrero@unice.fr
Université Côte d’Azur, CNRS, LEAT
Biot, France

Leonardo Lizzi

leonardo.lizzi@unice.fr
Université Côte d’Azur, CNRS, LEAT
Biot, France

Arnaud Legout

arnaud.legout@inria.fr
Université Côte d’Azur, Inria
Valbonne, France

ABSTRACT

From crowdsource data collection to automation and robotics, mobile smartphones are well suited for various use cases given the rich hardware components they feature. Researchers can now have access to various sensors such as barometers, magnetometers, orientation sensors, in addition to multiple wireless technologies all on a single and relatively cheap mobile smartphone. In this work, we study the performance of smartphones to measure cellular wireless power. We performed our experiments inside an anechoic chamber in order to compare the measurements of smartphone to the ones obtained with professional spectrum analyzer. We first evaluate the effect of orientation on the received power, then we propose a way to improve the accuracy of smartphone power measurements by using the orientation sensors. We improve the accuracy of the measurements from 25 dBm RMSE to no more than 6 dBm RMSE. We also show how we can exploit the characteristics of the reception pattern of the smartphone to determine the angle of arrival of the signal.

KEYWORDS

calibration, smartphone, wireless power measurement, IMU, LTE

1 INTRODUCTION

Recent years have witnessed an increase in the number of connected devices such as smartphones. This type of mobile devices embed more and more hardware, a decent computing power, a full set of sensors, and great wireless capabilities which make them accessible, and multipurpose computing devices. In contrast, professional measurements tools such as spectrum analyzers are not easily accessible. They are generally very expensive and hard to carry. Consequently, commodity COTS hardware in general and mobile smartphones in particular are getting more and more attention

in the research community to replace the specialized equipment, either for signal generation by using Software Defined Radio (SDR) [18] or for spectrum measurements [19][13][1].

In this work, we propose a commodity wireless power measurement solution that works on *any* COTS Android smartphone. We developed an algorithm that uses calibration matrices to calibrates the raw power measurements of the smartphone in order to approximate the real power that would be measured with a specialized spectrum analyzer. We validated our algorithm in different scenarios and in different transmission conditions. In all cases, we managed to approximate the real power with less than 6 dBm Root Mean Square Error (RMSE).

Using commodity hardware and smartphones for spectrum measurement was tackled in previous works. Tan et al. proposed *Snoopy* [19], a spectrum analyzer that uses commodity Wi-Fi cards with frequency translators to sense a wide range of frequencies. The Wi-Fi card normally scans only at 2.4 GHz and 5 GHz. To extend this range and scan a wider spectrum, Snoopy uses an RF frequency translator that senses and translates the signals to adapt them to the supported frequency by the Wi-Fi card. This is not readily applicable on COTS smartphones as they do not expose RF connectors of their Wi-Fi cards. Another work that aimed at using commodity smartphone as spectrum analyzer is presented by Ana et al. [13]. They used a portable Software Defined Radio (RTL-SDR) dongle that senses a continuous spectrum range from 52MHz to 2200 MHz, which they connect to a smartphone through USB. The dongle is the spectrum analyzer. The smartphone only processes the data from the dongle. In contrast to the two aforementioned works that rely on external hardware, CrowdREM [1] relies only on smartphones for spectrum analysis. The authors used an open source mobile phone (OpenMoko [15]) on which they installed a modified linux system and replaced the whole baseband system by OsmocomBB [16], another open source

GSM baseband implementation. They showed that smartphone accuracy is within 3 dBm while the device is still, but very sensitive to orientation with respect to the source, up to 10 dB difference.

As opposed to the previous works [19][13], the solution we propose in this paper relies solely on a smartphone without any other external hardware. Moreover, our solution doesn't require neither a hardware modification on the smartphone nor software modification (no rooting and no custom operating system required). We mitigate the inaccuracy of smartphones [1] with a calibration algorithm that uses the Inertial Measurements Units (IMUs) of the mobile device to determine the correction power offset to apply.

In this work, we present three major contributions.

- We show the feasibility of using unmodified, COTS smartphones without any external hardware to measure wireless power by making use of the orientation sensors to calibrate the measurements.
- We show how to determine the direction of the incoming transmitted signal from the source by using the characteristics of the reception pattern of the smartphone.
- All the calibration artifacts and measurements data are available to the community. The pre-computed calibration matrices are available as an Android mobile application for an easier reusability¹.

The rest of the paper is organized as follows. In section 2, we present some constraints affecting the design and placement of smartphone antennas and how this could impact the performances of these antennas. In Section 3, we present the experimental methodology we used to rotate a smartphone in space and collect the received power in different orientations. In section 4, we show the effect of changing the smartphone orientation on the accuracy of its received power measurements. Next, we present a calibration algorithm in section 5 that will correct the raw power measurements of the smartphone by compensating for the effect of orientation. In section 6, we evaluate our algorithm in different scenarios, and in section 7 we discuss the limitations. We conclude the paper in section 8.

2 SMARTPHONE ANTENNAS

Smartphones are widely used in wireless telecommunication. They support various telecommunication protocols such as cellular technologies (GSM, WCDMA, LTE), Wi-Fi and Bluetooth. All these protocols usually work at different radio frequencies, spanning from 800 MHz upto 5 GHz [11]. In

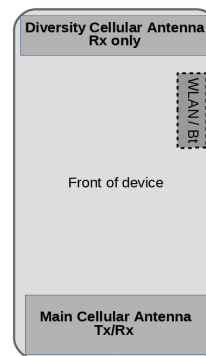


Figure 1: Location of antennas on smartphone.

order to support the aforementioned telecommunication protocols, different antennas are required on the device. A dedicated antenna for Wi-Fi, one for Bluetooth, one for both GSM and WCDMA, and multiple antennas for LTE. It is common to have multiple technologies working at the same time like streaming music to your Bluetooth headset while downloading a file using cellular data. This can cause a lot of interference between the antennas. That's why smartphone manufacturers tend to limit the number of antennas by making a multiband antennas that can be shared by more than one technology, like for example Bluetooth and Wi-Fi since they work on almost the same frequencies (around 2.4 GHz) [12].

Moreover, the design of an antenna depends mostly on the frequencies it will support. Antenna size is inversely proportional to the frequency: the lower the frequency, the bigger the antenna size. But the space constraints on modern smartphones makes it harder to fit all these antennas inside.

Also, smartphone manufacturers are obliged to design their antennas in such a way to limit the radiated power when transmitting. This is known as the Specific Absorption Rate (SAR) [11]. SAR defines the maximum power the antenna should not exceed in order to not cause biological damage when the device is put very close to the human body. That's why the transmitting antennas are generally put at the bottom of the device, further from the head while the receive-only antennas or diversity antennas are generally on the upper part. Most of smartphone manufacturers adopt the scheme depicted in Figure 1 for antennas placement.

Given all these design constraints, the architecture and the design of smartphone antennas will surely have an impact on their performances, as shown by Achtzehn et al [1], where the received signal power is easily affected by the device orientation. To verify this, we collected the reception pattern of the LG Nexus 5x cellular antennas along 3 axis inside an anechoic chamber (the detailed methodology is presented in section 3). The results are shown in Figure 2. As we can see,

¹All contributions will be given for the camera-ready version of the paper.

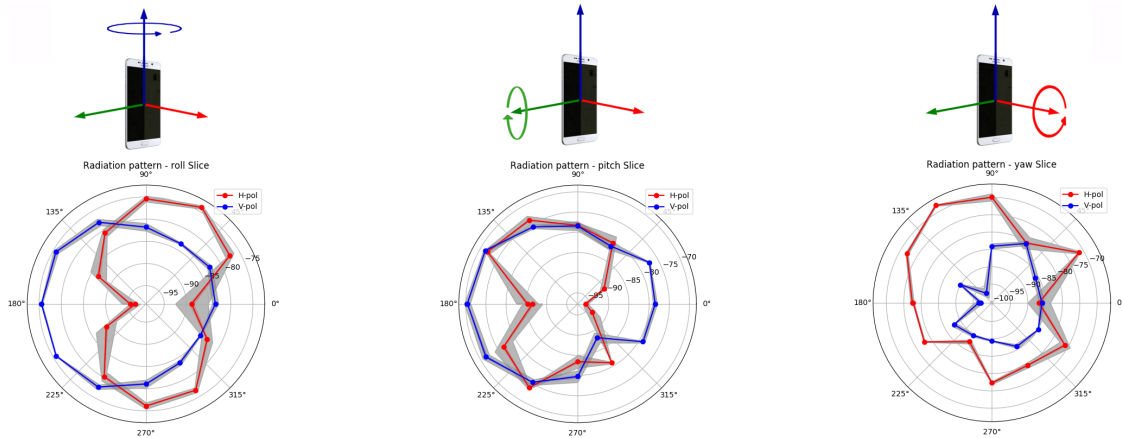


Figure 2: Reception pattern of the LG Nexus 5x in 3 planes: roll, pitch and yaw.

the received power changes depending on the orientation of the device and the polarization of the source. Also, we notice the duality between the reception patterns for the two polarizations. When the reception is optimal for a given polarization, the other gives lower performance. This may not always be the case as the reception performance depends on the antenna design and its symmetry with respect to polarization axis.

In the following sections, we study more the effect of orientation of the smartphone on the received power by taking the LTE network as a case study.

3 METHODOLOGY

3.1 Cellular signal generation

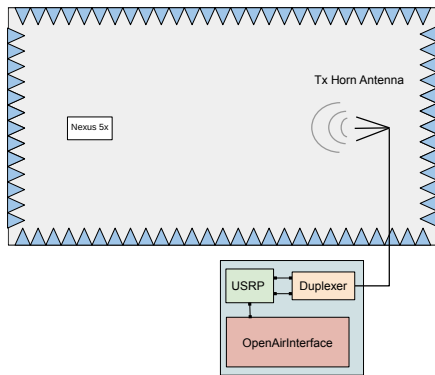


Figure 3: The experimental setup. The 2.6 GHz LTE cellular network is generated using OpenAirInterface, USRP and a transmitting horn antenna.

We use an LTE network for our experimentation. We rely on Software Defined Radio (SDR) [18] to generate the signal. OpenAirInterface (OAI) [14] is an open-source, complete,

software implementation of an LTE cellular network that can run on general purpose processors. We installed OAI on a single laptop machine, running Ubuntu 16.04 LTS, with Intel i7-6th-gen processor, with 32 GB of RAM.

We connect the laptop to an Ettus B210 Universal Software Radio Peripheral (USRP) [10] for which we use duplexer to connect it to the transmitting antenna (Figure 3). The transmitting antenna is the ETS-Lindgren’s 3115 double-ridged horn antenna [9]. It is a directional antenna with linear polarization having a gain of 9.9 dBi at 2.5 GHz. It supports a wide range of frequencies ranging from 750 MHz to 18 GHz. We use LTE band 7, 2.6 GHz, and an LG Nexus 5x smartphone running Android 7.1 with a pre-programmed SIM card to connect to the test network.

3.2 Controlled environment

We perform our experimentations in an anechoic chamber that has a programmable robotic equipment both at the transmission and the reception sides. As shown in Figure 4, the reception platform is a two-axis positioners system that rotates along two axis: φ (Azimuth, angle between x and z axes) and θ (Roll, angle between y and z axes). φ can rotate 180 degrees (from -90 to +90) whereas θ can make 360-degrees rotation. The transmission platform (on the right of Figure 4) can only rotate along θ . It is located at $\varphi=0$. By combining the two-axis rotations, we can obtain measurements of the received power of the smartphone in different orientations in space. The reception and transmission are separated by a distance of 4 meters.

The two platforms are connected to a controller system outside of the chamber that allows us to program the rotation of the platforms by defining the rotation range, the step, and the time duration it remains at each orientation.

3.3 Collecting the logs

For the smartphone log collections, we use the Electrosmart application [8]. Electrosmart is an Android mobile application dedicated for measuring the radiations emitted by telecommunication infrastructures. It can measure all cellular technologies (GSM, WCDMA and LTE) in addition to Bluetooth and Wi-Fi signals. It makes use of Android API calls to get readings from the device antennas and orientation sensors to take measurements of the received power and the device's orientation in space, respectively. We instrumented the application to collect the logs every 1 second.

The controller of the anechoic chamber creates time-stamped logs of the values of its axes of rotation each time it reaches a programmed orientation.

The clocks of both the smartphone and the controller are synchronized each time we start an experiment.

3.4 Types of logs

All the logs are either stored on the smartphone for the smartphone logs or on the controlling computer of the anechoic chamber for the two-axis positioner logs.

The smartphone logs contain the received power and the device orientation.

The received power in case of LTE signal is called RSRP which is a negative integer that ranges from -140 to -44. The RSRP is represented in a logarithmic scale of power called dBm, where 1 dBm = 1 mWatt. The received power is obtained by calling the NetworkManager APIs of Android.

3.4.1 Getting the received power on Android. The Android Application Programming Interfaces (APIs) offer two possibilities to get the received power by the device. One method consists of registering a listener that will generate a callback whenever there is a change in the signal strength. The other one is an explicit request to the operating system to retrieve the received power (or signal strength). We detail them in the following.

- **PhoneStateListener:** is a callback-based methods available on Android under the *telephony* package to monitor the signal strength, that require registering a listener for specific events (for example, changes in the signal strength). So by registering a listener to monitor the changes in the network signal strength, it will invoke a callback whenever the signal strength changes [6].

- **getAllCellInfo():** is another way to get the network signal strength is to make an explicit call to the operating system by invoking the *getAllCellInfo()* method (available under the *TelephonyManager* class) to fetch the most recent signal strength known to the hardware [7].

The two methods are supposed to report the change in the signal strength of the network. But what about their

performances? Do they have the same sensitivity? Which one is better to monitor the changes in the signal strength?

In order to compare the performance of the two methods available on Android to get the network signal strength, we put an LG Nexus 5X smartphone at the reception side of the anechoic chamber in front of a source, as shown in Figure 4. Then, we vary the transmission between -45 dBm and -20 dBm with a step of 1 dB every minute. We record the received power on the smartphone using the two aforementioned methods. We trigger a call to *getAllCellInfo()* every 1 second. The results are shown in Figure 5.

The method *getAllCellInfos()* is more sensitive to the change in the received signal than the *PhoneStateListener* method. For example, at time 10h45, *PhoneStateListener* keeps giving the same power (-80 dBm) regardless of dropping the transmission power from -20 dBm to -25 dBm, then it suddenly updates to -85 dBm. In contrast, *getAllCellInfos()* follows exactly the updates in the transmission power.

For the rest of this work, we choose *getAllCellInfos()* to measure the received power on the smartphone.

3.4.2 Getting the smartphone orientation on Android. The orientation of the smartphone is obtained using another Android APIs, called Rotation Vector Sensor (RVS). It is a software sensor that combines many hardware sensors readings (Accelerometer, Magnetometer and Gyroscope) to estimate the device's orientation in space. The RVS, as its name suggests, returns a vector from which we can extract a normalized quaternion of orientation. Quaternion[5] is a mathematical representation of orientation. Quaternions are 4 dimensional complex vectors in a form of $[w, x, y, z]$, where w is the real part that represents the magnitude; x, y, z are the imaginary parts that corresponds to each axis in the 3D space. Quaternions can be averaged by interpolation, known as *slerp* [5] (Spherical Linear interPolation) and, in contrast to Euler angles, they do not suffer from Gimbal lock [2].

The program that controls the two-axis positioner generates logs containing each axis angle (in degrees) of both the reception and transmission positioners. A separate text file is created for every programmed orientation with a corresponding timestamp. These logs are solely used as ground truth values for device orientation inside the chamber and also to group the smartphone logs for each programmed orientation.

3.5 Experimental limitations

For measurements acquisition, we faced some limitations.

First, the received signal strength from the smartphone does not have a high refresh rate (around 1 second at best). It is due to power optimization by restricting the number of messages exchanged between the device's baseband (which

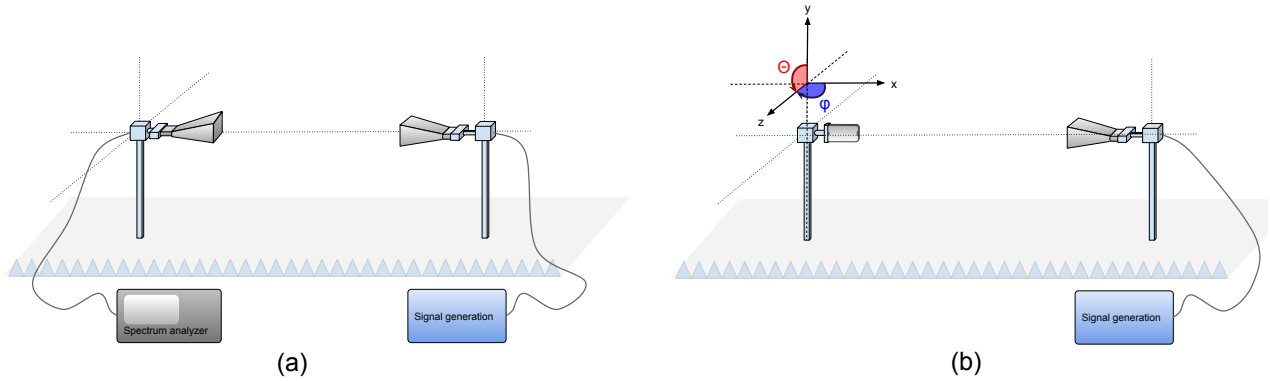


Figure 4: (a) We first measure the reference power using a spectrum analyzer, then (b) compare it with the raw measurements obtained from a COTS smartphone at 665 different orientations by rotating it along two axis φ and θ : φ makes 180 degrees rotation at a step of 10 degrees, for each value of φ , we change θ from 0 to 350 degrees at a step of 10 degrees.

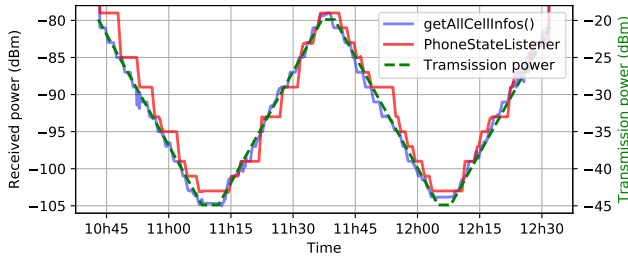


Figure 5: Comparing Android API calls to get the cellular received power. `getAllCellInfos()` method is more reliable and more sensitive to change in the signal strength than the `PhoneStateListener` method.

has a higher refresh rate) and the Android OS. Higher refresh rate would have shortened the time spend on collecting the calibration data.

Second, the two-positioner system can only rotate along two axis, which means we cannot test all the relative orientation of the device with respect to the source. This can be solved by rotating the source itself along φ . We limit our study on subset of relative orientations of the smartphone to the source by considering two polarizations of the source (horizontal and vertical polarization), and all the details of the calibration process we present in this work can be replicated on any other orientations or polarizations without loss of generality.

4 SMARTPHONE POWER MEASUREMENT ACCURACY AND EFFECT OF ORIENTATION

In this section, we evaluate the accuracy of the smartphone’s raw measurements of signal strength inside an anechoic

chamber, and quantify any effect of smartphone’s orientation with respect to the source on the received power.

4.1 Measuring the reference power

First, we measured the real power at the reception using a Rohde-Schwarz FSL3 spectrum analyzer [17]. We use a horizontal polarization at the source. We mount on the spectrum analyzer a horn antenna identical to the transmitting antenna with the same polarization as the source (Figure 4(a)). By removing the antenna gain (10 dB) and compensating for cable loss (1 dB), the power measured at the reception is **-54 dBm**. We call this power *the reference power*.

4.2 Sensitivity to orientations

We want to know how close the measured power by a COTS smartphone is from the reference power. To do so, we replace the horn antenna at reception with a smartphone as shown in Figure 4(b). In order to study the effect of the mobile phone’s orientation on the received power, we put the device in 665 different orientations in space along two axis: φ and θ directly in front of the transmitting antenna, as illustrated in Figure 4 (b). At each position, we collect the received power and the device orientation.

We keep the device at each orientation for 5 seconds, this allows the mobile application to collect about 5 tuples of (power, orientation). We then average these tuples into one tuple of (power, orientation). Power averaging is done in linear scale (Watt) and the result is converted back to logarithmic scale (dBm). The orientation is obtained by sleeping quaternions and expressed as a normalized quaternion with magnitude equals to 1 to represent the smartphone orientation in space and keep track of orientation effect on the received power.

To verify the stability of the received power at each orientation during the 5 seconds of measurements, we calculated the standard deviation of power at each orientation. The mean standard deviation of powers in all the 665 orientations was only 0.06 dBm.

Moreover, to verify the reproducibility of the measurements in the controlled environment, we repeated the same experiment 10 times. For every experiment, we start the experimental process from scratch: we set up the cellular network, we calibrate the orientation sensors smartphone [4], we position it on the two-positioner system, then launch the controller program to start rotating the device and collect the measurements. We computed the mean standard deviation of the received power at each orientation in all experiments is 0.51 dBm. We also computed the mean angle error for each orientation in the 10 experiments. The results are depicted in Figure 6. Overall, we have a mean angle error of 5.5 degrees. The error varies depending on the orientation. Most orientations have low angle error and few of them have up to 13 degrees. The angle error is due to the accuracy of the hardware sensors embedded on the device, which could be impacted by the quality of the sensors or any electromagnetic interference from the anechoic chamber apparatus's motors. However, we consider this level of precision good enough for our study.

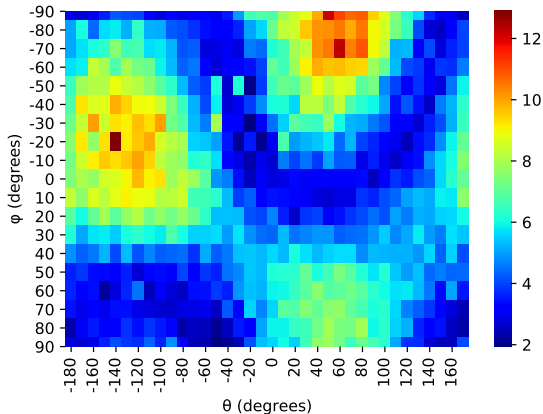


Figure 6: Mean angle error (in degrees) in all 665 orientations. Overall, the error is very low and less than 10 degrees in most orientations. Few orientations give more than 10 degrees error.

We merged all 10 experiments and for each orientation, we compute the average power and the mean quaternion using quaternion sleeping. For the rest of our study, we consider using the resulting averaged powers and orientations.

Figure 7 (a) shows a heatmap of the resulting received signal power in all 665 orientations with horizontal polarization of the source.

We clearly see the variability of the received signal strength between different orientations. The optimal power we measured was -70 dBm at $\theta = +90$ and $\varphi = 0$ (same orientation as depicted in Figure 4(b), which is 16 dB less than the reference power. At some orientations, the performance of the receiving antennas is very poor with a minimum of -92 dBm.

We evaluated another polarization of the source (vertical polarization) by repeating the same measurement process performed for the horizontal polarization. The resulting received power for the same 665 orientations are shown in Figure 7 (b). Again, we see the variability of received power with an offset of 18 dBm between the maximum and the minimum received power by the smartphone. These results are expected given the small size of smartphone antennas and their design in addition to the smartphone casing. *Hence, the smartphone cannot precisely measure the real power out-of-the-box.*

For the rest of this work, we consider only the horizontal polarization of the source. The study can easily be replicated to any other polarization without loss of generality.

Next, we explore the orientations that minimize and maximize the received power. In antenna theory, *Polarization Matching* [3] (or co-polarization) means that the receiver and transmitter have the same polarization, and the power loss is minimal. In contrast, cross-polarization yields minimal power. To verify whether we can detect polarization matching and cross-polarization with smartphones, we plotted the mean received power along the two axis of rotation in Figure 8. Along θ axis, the maximum power is received when the smartphone is in the main lobe of transmission ($\theta = 0$). We also see that the maximum power along φ is at ± 90 degrees, and lowest when the smartphone is perpendicular to the source polarization. Hence, smartphone antennas are affected by their relative orientation with respect to the source and the optimal performance is observed when its polarization matches the polarization of the source.

In conclusion, *COTS measure a lower power than the reference power and the measured power is affected by the orientation of the smartphone in space.* In the next section, we mitigate these two issues by calibrating the received power, that is, obtaining a measured power close to the real power and independent from the smartphone orientation.

5 CALIBRATION

5.1 Calibration technique

In order to calibrate the received signal strength, we make use of the embedded sensors of the smartphone to capture the orientation in space combined with the raw received power. The idea is to make lookup tables or matrices for orientations and power, from which we determine the correcting factor to apply at a given orientation.

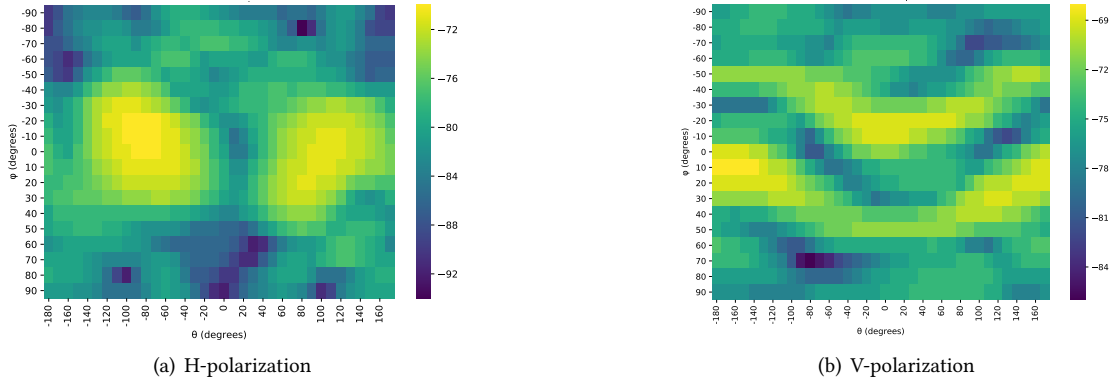


Figure 7: Heatmap of received signal strength (in dBm) by the LG Nexus 5X for 665 orientation with two polarization of the source (a) For Horizontal polarization, the maximum received power is -70 dBm, which is 16 dB below the reference power, and variability of the received power up to 24 dB between minimum and maximum received power. (b) For Vertical polarization, we observe a maximum power of -68 dBm and an offset of 18 dB between maximum and minimum received power.

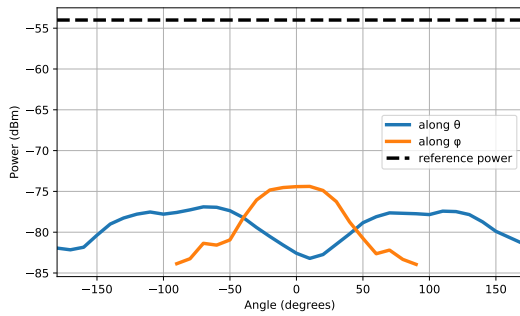


Figure 8: Mean received power along ϕ and θ . The received power is optimal when the antenna is in co-polarization with the source ($\phi = \pm 90$) and when the smartphone is directed towards the source ($\theta = 0$)

Let Q be a matrix of orientation Quaternions, and let P , another matrix having the same dimensions as Q , be a matrix of Power. We call them calibration matrices. We rotate the smartphone as shown in Figure 4(b). For each orientation, we fill up the matrix Q with the measured quaternion, and the matrix P with the offset between the raw measured power at that orientation and the reference power we measured beforehand in section 4.1 using the spectrum analyzer. In other words, each cell in the matrix Q contains a quaternion representing a given orientation. In each cell of matrix P , we put the difference between the reference power and the raw measured power at the orientation described by a quaternion in Q at the same coordinates. The calibration process is summarized in Figure 9.

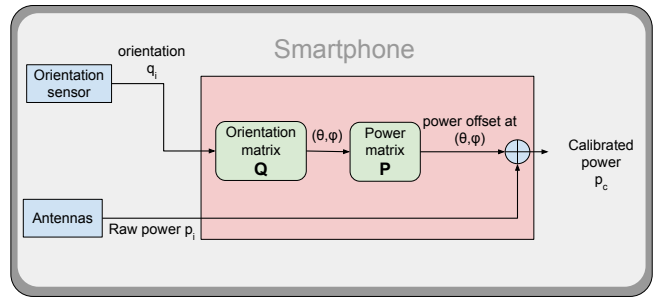


Figure 9: Calibration process. The smartphone measures the power p_i and the orientation q_i . From Q we find the closest calibrated orientation and its coordinates (θ, ϕ) , P gives us the corresponding calibration offset at the same coordinates, which is then added to the raw power p_i to get the real power.

Once we have these two matrices, whenever we put a device in a given orientation defined by a quaternion q_i , we compare it to every quaternion in Q and compute the relative angle. The closest quaternion in Q gives us the minimal angle. We use its coordinates in Q to obtain the corresponding correction offset from P to apply it on the raw measured power in order to calibrate it.

Performance-wise, quaternion lookup and comparison in Q has linear complexity. The performances can be improved by using hashing data structures for faster lookup. For this work, we settle for the linear approach and consider the optimization in future works.

5.1.1 Building the calibration matrices P and Q . The first step is to build the calibration matrices and use them as

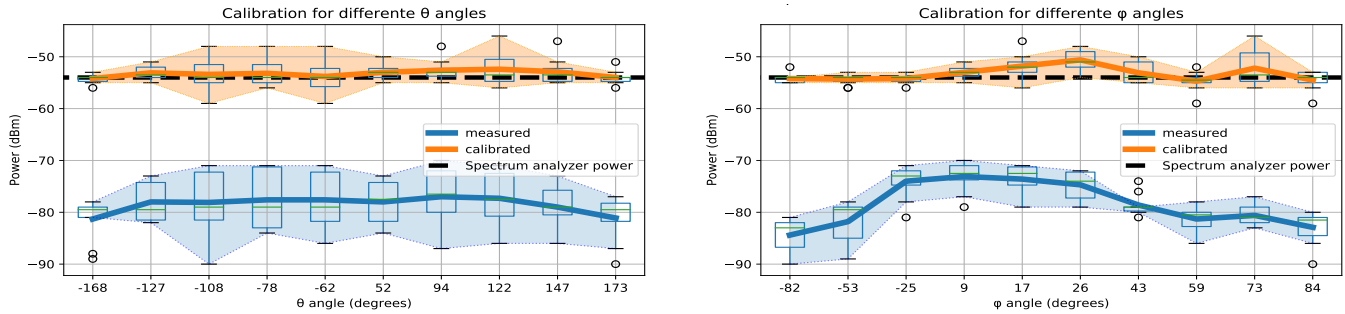


Figure 10: Boxplots for calibration results of the 100 random orientations along θ and φ . The calibrated signal (orange) is closer to the reference power (black dashed line), and less variable compared to the raw measured signal (in blue). The shaded area represents the variability range of measurements. The RMSE for the calibrated values is 2.37 dBm compared to 25 dBm error for the raw measurements.

lookup tables to determine which correction offset to apply on the received power. To do this, we rotate the smartphone as depicted in Figure 4(b). We initially put the device at $\varphi = -180$, and $\theta = -90$. Then, we move φ from 0 to 350 degrees with steps of 10 degrees. We do that for every θ that goes from -90 to $+90$ with step of 10 degrees. At each step, we collect the received power and rotation quaternion. Then, we insert them in the matrices with the corresponding φ and θ coordinates.

5.1.2 Post processing. At the end of each experiment, we obtain the smartphone logs containing the received power, the rotation quaternions and their timestamps. We also extract the generated logs of the rotating apparatus of the anechoic chamber containing the exact orientation of the reception platform (hence, the smartphone) and the timestamp it reached this orientation. The apparatus logs record the values of φ and θ which are used as a coordinates when filling the calibration matrices. The apparatus logs also contain timestamps which are used to filter the smartphone logs for each orientation.

We put all log files in one folder then run a script we wrote that reads, extracts and filter the logs to generate the two calibration matrices, P and Q .

5.2 Calibration

Now that we obtained the calibrating matrices, can we calibrate any other random orientations? To test this, we generated 100 random orientation by taking 10 random values for φ and θ in the ranges $[90, +90]$ and $[-180, 170]$ respectively in such a way that the random orientations are not in Q . The transmission parameters are kept the same.

The received power and the orientation are collected and processed as explained in section 4.2.

The calibration is applied as follows: for every random orientation, we compare the corresponding quaternion to

every quaternions in Q to get the closest quaternion and its coordinates. We use these coordinates to determine the power offset to add to the measured power to calibrate it, see Figure 9.

Applying this process on 100 random orientation gives the results depicted in Figure 10. The calibrated power is very close to the reference power measured by the spectrum analyzer, as opposed to the raw measurement, which feature a high variability and is much below the reference power. To quantify the quality of the calibration, we use the Root Mean Square Error (RMSE) between the calibrated signal and the reference power. RMSE is defined in Equation 1.

$$RMSE = \sqrt{\frac{\sum_{i=1}^N (Reference\ power - Calibrated\ power_i)^2}{N}} \quad (1)$$

Where N in Equation 1 represents the number of orientations we tested (In this case, $N = 100$).

The RMSE for the calibration is only **2.37 dBm** compared to **25 dBm** RMSE for non-calibrated measurements. This shows that our calibration process gives a satisfying results that compensate for smartphone antenna performances and the effect of orientation on the received power.

6 ADAPTING CALIBRATION FOR UNKNOWN SOURCE CHARACTERISTICS

In section 5, we studied the effect of device orientation in space on the received signal strength. We showed how we can calibrate the measurements to compensate this effect. Up to now, the location of the source is supposed to be known. What will happen if the source is moved, or the transmission power is changed? Can we find the new location the source and reuse the calibration matrices obtained before?

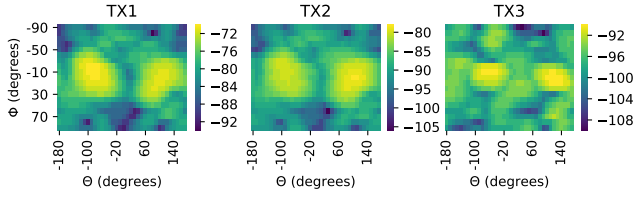


Figure 11: The received power by the Nexus 5X for different transmitted power

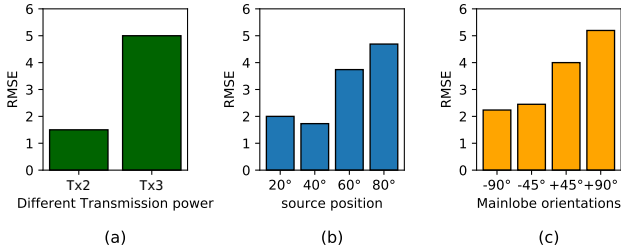


Figure 12: Calibration errors when the source configuration changes. We manage to reuse the calibration matrices we obtained earlier to calibrate the measured signal with an error less than 6 dBm even if the source changes position.

In this section, we evaluate our calibration technique against a change in the transmitted power or a change of the source location with respect to the smartphone. Then, we verify to which extent the calibration matrices are still valid. To simplify the study, we assume that the source polarization does not change and is known beforehand, knowing that we can still estimate the polarization using the property of polarization matching, as explained in section 4.2. Without loss of generality, we only consider changing the source location along the azimuth axis (θ).

6.1 Calibration for unknown transmission power

First, we consider the case where the source does not change its position with respect to the smartphone and keeps the same position as when we collected the calibration matrices, as depicted in Figure 4 (b). We reduced the transmitted power twice with 10 dB difference each time by using signal attenuators to obtain two different powers (TX2 and TX3). For each transmitted power, we measure the reference received power as explained in section 4.1. We measure -64 dBm and -74 dBm for TX2 and TX3, respectively. For each transmitted power, we collect measurements with the same process as described in section 5.1 by rotating the smartphone along θ and φ . The resulting received patterns are depicted in Figure 11.

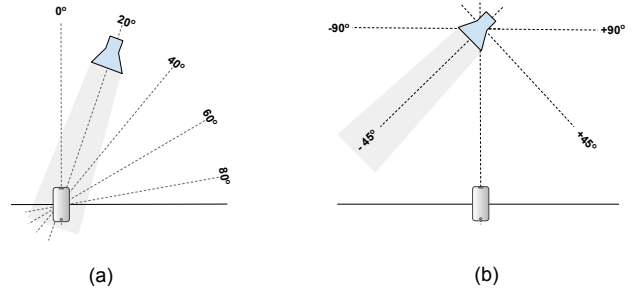


Figure 13: (a) Changing the source’s position with respect to the smartphone. (b) Pointing the source’s main lobe at different angles with respect to the smartphone.

Now, can we calibrate those measurements using the calibration matrices? We apply the calibration process on both cases and compute the error to the reference powers (-64 dBm and -74 dBm). The results are shown in Figure 12(a).

The errors are 2 and 5 dBm for TX2 and TX3, respectively. Again, for TX2 we obtained a lower error compared to TX3, which is due to the distortion in the received pattern for TX3. *Our calibration technique is able to calibrate the received power for different transmitted powers using the same calibration matrices with an error of no more than 5 dBm.*

6.2 Calibration for aligned source with unknown position

Now, let’s consider the case where the source’s location with respect to the smartphone is unknown. How does this affect the received pattern of the smartphone and how can we calibrate a signal coming from an unknown direction? In this experiment, we put the transmitting antenna at different azimuth (φ) angles around the smartphone while keeping the smartphone inside the main lobe of transmission. We then test whether we can reuse again the calibration matrices to calibrate the received power.

As shown in Figure 13 (a), we rotate the source at 20, 40, 60 and 80 degrees from the original orientation shown in Figure 4 (b). We precisely position the source using a laser beam and axis value readings from the rotating apparatus of the anechoic chamber to make sure that the source is shifted by the correct angle. At each new position, we measure the reference power using a spectrum analyzer.

Figure 14 shows the received power patterns for all the tested angles. The patterns seem to be a shifted version of the reception pattern at 0 degrees. To verify and validate this, we make a correlation plot between them and the measured pattern at 0 degrees. This is shown in Figure 15. We see that the reception patterns are highly correlated at exactly 20, 40, 60 and 80 degrees shift with respect to the measurements at 0

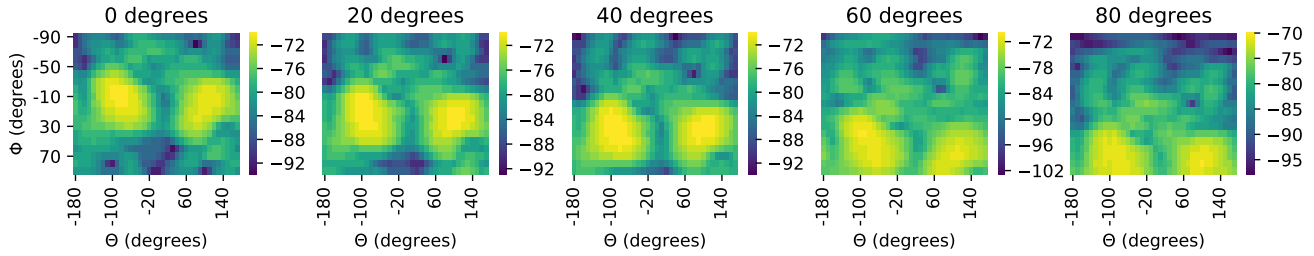


Figure 14: The received power by the Nexus 5X when the source is put at different angles. The reception pattern are a shifted versions of pattern at 0 degrees with the corresponding angle change in source position.

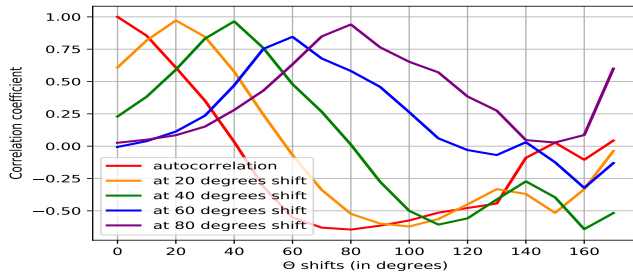


Figure 15: Correlation plots. The reception patterns are highly correlated with the pattern at 0 degrees with shifts corresponding to the new source position.

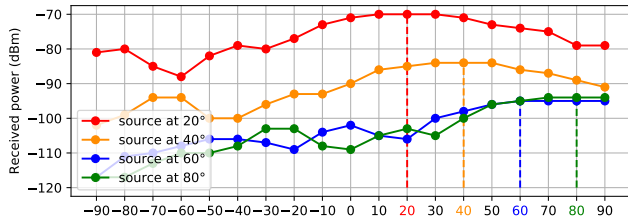


Figure 16: Sweeping along φ axis to locate the source. The Source is located where the maximum power is measured.

degrees. Hence, the reception pattern is preserved regardless of the source position with respect to the smartphone.

Now that we showed the preservation of the reception pattern even if we move the source and change its location, it means we can reuse our calibration matrices we collected when the source was at $\varphi=0$ degrees in order to calibrate the received power when the source is at different angles with respect to the smartphone. To do so, we first need to locate the new position of the source, then define the angle shift from $\varphi=0$ position to the new source position. Then, we translate the calibration matrix of orientation Q to adapt it to the new source position.

To locate the source, we use the property of antennas polarization we explained in section 4.2, where the reception is maximum when both the transmitting and the receiving antennas are aligned and co-polarized, i.e., they have the same polarization. So, by knowing the polarization at transmission, we put the smartphone in the same polarization, then we sweep along φ and collect the received power. The source will be located when we measure the maximum power at an angle $\varphi = \varphi_x$.

The smartphone receives more power when θ is $+90$ or -90 degrees, as illustrated in Figure 8. So we put the smartphone at $\theta = +90$, then we rotate the phone along φ axis from -90 degrees to $+90$ degrees and collect the received power at each value of φ . The results are plotted in Figure 16. The received power increases gradually as we point the smartphone closer the new source location. The maximum power is received when the smartphone is directly aligned with the source along the azimuth (φ).

After we locate the source, we need to transform and shift the matrix of orientation quaternions Q to adapt it to the new source change. We apply quaternion rotation using the relative quaternion describing the rotation from $\varphi = 0$ to $\varphi = \varphi_x$, the new source position in the azimuth.

Now that we adapted the calibration matrices to the change in source position, we can calibrate the received power. The RMSE between the calibrated and the reference power are plotted in Figure 12(b) for all tested source positions. The RMSE is below 5 dBm in all cases. *We conclude that we can calibrate the smartphone measurements from a source with unknown location along the azimuth.*

6.3 Calibration outside the main lobe of transmission of a source with known position

Previously, we considered the calibration when the source position or transmission power is unknown and the smartphone was in the main lobe of transmission of the source. What will happen to the received signal power when the

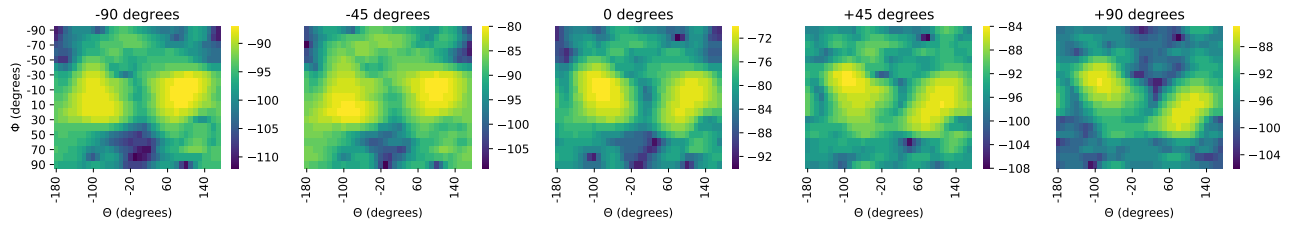


Figure 17: Heatmap of the received pattern by the Nexus 5X when the main lobe is oriented in different direction.

smartphone is no more inside the main lobe? Can we still calibrate in that case?

In this section, we study the received power when the smartphone is not directly targeted by the main lobe of the transmitting antenna. As shown in Figure 13 (b), we point the main lobe at different angles with respect to the smartphone. At each angle, we rotate the smartphone along φ and θ to collect the received power.

Figure 17 shows the heatmap of the received power by the smartphone in all tested cases. The maximum power is received when the smartphone is co-polarized with the source (at $\pm 90^\circ$ θ degrees) and directed towards it (at $\varphi = 0$).

Now, can we still reuse the calibration matrices P and Q to calibrate the received power when the source’s main lobe is not directed towards the smartphone?

No transformation is required on the calibration matrices since the source is aligned with the smartphone along the azimuth as in shown in Figure 4.

We apply the calibration process described in Section 5.1 for each case of source rotation. First we measure the reference power with a spectrum analyzer, then we put the device in the same 665 orientations and apply our calibration matrices P and Q to calibrate the measurements.

The RMSE for the calibrated signals in all cases are shown in Figure 12(c). Again, we see that the RMSE is within 5 dBm. *This shows that the calibration still works even if the smartphone is not directly in the main lobe of transmission.*

7 DISCUSSION AND LIMITATIONS

7.1 Calibrate once, runs everywhere

The main advantage of our calibration solution is that it can be easily distributed as a mobile application that can be installed on any Android smartphone for wireless power measurement. Once we build the calibration matrix of a given smartphone, we embed it inside an Android application, which can then be distributed on other smartphones of the same brand and model to turn them into a ready-to-use wireless power measurement tool ².

² All the raw measurements, calibration matrices and scripts used in our study are provided to the community.

7.2 Measurable signals

Our calibration methodology is only applicable for measuring the received power from protocols that are supported by the smartphone. It cannot be applied to measure the wireless power of non-supported technologies. So for example, we cannot measure and calibrate the transmitted power of other smartphones while they communicate with the core cellular network. This limits our work to a subset of signals but given the fact that we wanted to have a calibration solution that can run on any Android smartphone without any software or hardware modification, and without relying on external hardware allows us to harness the power and affordability of millions of devices and use them as a low cost, commodity hardware solution for wireless power measurement.

7.3 Outdoor, multipath and polarization diversity

We did our study inside a controlled environment with a direct line of sight between the source and the reception, with a single polarization at the transmission. In outdoor scenarios, the environment is more dynamic with many reflections and multipath effect. Moreover, the base stations nowadays use transmission diversity, like spacial diversity and polarization diversity where the signal is transmitted at two perpendicular polarizations from an antenna array in order to improve cellular reception. Polarization diversity gives a gain of up to 12 dB compared to single polarization [11]. A typical sector antenna’s interior is depicted in Figure 19.

To assess the effect of orientation of the received power by the smartphone in outdoor environment, we put the LG Nexus 5x smartphone, that we used in our study, in 88 different orientations, which are a subset of the 665 orientations we tested in the controlled environment, in direct line-of-sight with an LTE eNodeB, at a distance of about 170 meters (Figure 18(a)). We locked the smartphone to the same band we used in our study, band 7. The orientations are again described in terms of φ and θ . We distributed the 88 orientations on the two axes φ and θ to test different relative orientations between the smartphone and the source. At each orientation, we collect at least 20 measurement samples

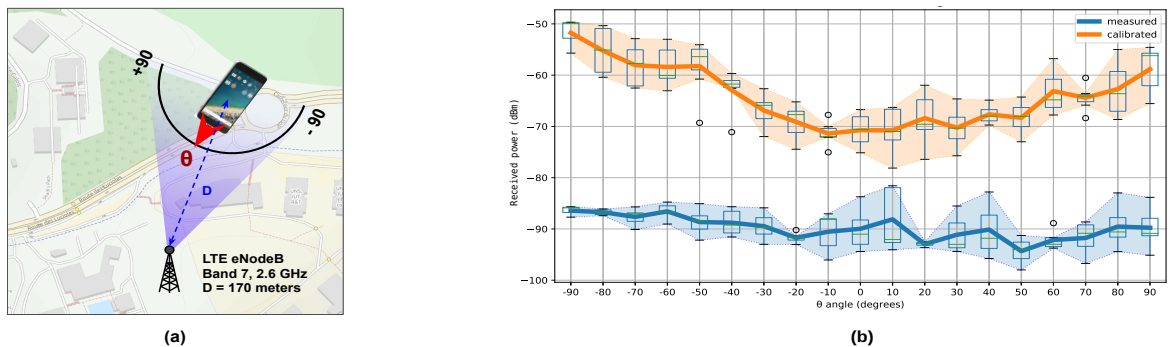


Figure 18: Outdoor calibration. (a) We put the smartphone in the main lobe of transmission of an LTE eNodeB, at a distance of 170 meters, then we put the device in 88 different orientations along φ and θ . (b) The calibration results of outdoor measurements. The polarization diversity used at transmission allows the device to receive almost the same level of power regardless of orientation (in blue), and the calibration did not perform well (plotted in orange).



Figure 19: Interior of sector antenna (MIT Computer Science & Artificial Intelligence Lab). An array of dipole antennas in a "+" configuration to transmit the same signal on two perpendicular polarizations in order to minimize polarization mismatch at reception. Hence, improves cellular reception.

of the received power, we then applied the calibration matrix on the measurements. The results are shown in Figure 18(b).

The raw received power (shown in blue) on Figure 18(b), is less variable than what we obtained in the anechoic chamber (see Figure 10), across the 88 different orientations. The power offsets we defined in the calibration matrix P do not match the outdoor measurements, resulting in the variability of the calibrated measurements (shown in orange on Figure 18(b)).

By transmitting the same signal at two perpendicular polarizations (vertical and horizontal polarization), the smartphone antennas have higher chance to be in the same polarization with the transmission by receiving from either polarization. So the polarization diversity used at transmission

minimizes the chance of polarization mismatch (or cross-polarization). Hence, the effect of orientation on the received power in outdoor environment is minimized (low directivity), and *smartphones can be safely used outdoor for wireless power measurement without worrying about the orientation.*

8 CONCLUSION

In this work, we presented a novel method to use ordinary smartphones for wireless power measurements without any external hardware. We first studied the effect of relative orientation of the smartphone with respect to the source and compared the raw measurements of power to the real power obtained with specialized spectrum analyzer. We developed an algorithm that uses the Inertial Measurement Units (IMUs) of the smartphone to calibrate the receive power to the real power. Finally, we showed how we can calibrate even if the source location or transmission power is unknown with an RMSE less than 6 dB from the real power.

The calibration process presented in this work can open the doors to a cheaper solution for power measurement and can potentially transform millions of affordable devices into wireless power measurement tools.

REFERENCES

- [1] Andreas Achtzehn, Janne Riihijärvi, Irving Antonio Barriá Castillo, Marina Petrova, and Petri Mähönen. 2015. CrowdREM: Harnessing the power of the mobile crowd for flexible wireless network monitoring. In *Proceedings of the 16th International Workshop on Mobile Computing Systems and Applications*. ACM, 63–68.
- [2] A Alaimo, V Artale, C Milazzo, and A Ricciardello. 2013. Comparison between euler and quaternion parametrization in uav dynamics. In *AIP Conference Proceedings*, Vol. 1558. AIP, 1228–1231.

- [3] Constantine A Balanis. 2016. *Antenna theory: analysis and design*. John Wiley & Sons.
- [4] calibrateMag. 2019. *Calibrating magnetometer sensor*. ww2.mathworks.cn/help/supportpkg/beagleboneblue/ref/calibratemag.html
- [5] EB Dam, M Koch, and M Lillholm. 1998. Quaternions Interpolation and Animation. Datalogisk Institut. *Københavns Universitet* (1998).
- [6] Android Developers. 2019. *PhoneStateListener*. <https://developer.android.com/reference/android/telephony/PhoneStateListener>
- [7] Android Developers. 2019. *TelephonyManager*. [https://developer.android.com/reference/android/telephony/TelephonyManager.html#getAllCellInfo\(\)](https://developer.android.com/reference/android/telephony/TelephonyManager.html#getAllCellInfo())
- [8] ElectroSmart. 2019. *The first app to find your electromagnetic exposure*. es.inria.fr
- [9] ETS-Lindgren. 2019. *3115 Double-Ridged Guide Antenna*. www.ets-lindgren.com/products/antennas/double-ridged-guide/4002/400203
- [10] Ettus. 2019. *Ettus USRP B210*. www.ettus.com/product/details/UB210-KIT
- [11] Kyōhei Fujimoto. 2001. *Mobile antenna systems handbook*. Artech House.
- [12] Sampson Hu and David Tanner. 2018. Solving the antenna paradox: Adding more antennas to your smartphone creates more noise, but 3D manufacturing will fix the problem. *IEEE Spectrum* 55, 11 (2018), 40–45.
- [13] Ana Nika, Zengbin Zhang, Xia Zhou, Ben Y Zhao, and Haitao Zheng. 2014. Towards commoditized real-time spectrum monitoring. In *Proceedings of the 1st ACM workshop on Hot topics in wireless*. ACM, 25–30.
- [14] Navid Nikaein, Raymond Knopp, Florian Kaltenberger, Lionel Gauthier, Christian Bonnet, Dominique Nussbaum, and Riadh Ghaddab. 2014. OpenAirInterface: an open LTE network in a PC. In *Proceedings of the 20th annual international conference on Mobile computing and networking*. ACM, 305–308.
- [15] OpenMoko project. 2019. *OpenMoko*. www.openmoko.org
- [16] OsmocomBB project. 2019. *OsmocomBB*. osmocom.org/projects/baseband
- [17] Rohde&Schwarz. 2019. *FSL3 Spectrum Analyzer*. www.rohde-schwarz.com/fr/produit/fsl-page-demarrage-produits_63493-8042.html
- [18] Walter HW Tuttlebee. 1999. Software-defined radio: facets of a developing technology. *IEEE Personal Communications* 6, 2 (1999), 38–44.
- [19] Tan Zhang, Ashish Patro, Ning Leng, and Suman Banerjee. 2015. A wireless spectrum analyzer in your pocket. In *Proceedings of the 16th International Workshop on Mobile Computing Systems and Applications*. ACM, 69–74.